scientific reports

Check for updates

OPEN

Identification of candidate nsSNPs of the human *FNDC5* gene and their structural and functional consequences using in silico analysis

Sadaf Majeed[1,7], Hira Moin[2,7]✉, Maaz Waseem[3,6], Zoya Khalid[4]✉, Sumra Wajid Abbasi[5] & Kashaf Rasool[3]

***Fibronectin type-III domain containing protein-5 (FNDC5)*, predominantly expressed in skeletal muscles, encodes FNDC5 transmembrane-protein. A segment of this protein is cleaved and secreted into blood as irisin, which promotes browning of white adipose tissue, leading to energy expenditure. It functions synergistically with fibroblast growth factor-21 (FGF21). Irisin is considered as a potential target for treating obesity-related disorders. Likewise, *FNDC5* variations can contribute to development of such disorders. This study aimed to identify putative non-synonymous single nucleotide polymorphisms (nsSNPs) of human *FNDC5*, potentially impacting FNDC5-FGF21 interaction. Sequence and structure based computational tools were used to identify nsSNPs of *FNDC5*, which revealed eight nsSNPs as being most deleterious (N39K, R78H, R209H, T124I, L150P, L156V, V83M, and T86I). Molecular-docking was performed to analyze the impact of *FNDC5* mutations on wild-type and mutant FNDC5-FGF21 complexes, revealing that T124I (rs185141197) and L150P (rs377741902) showed higher buried surface area (BSA) than wild-type. Following this, molecular dynamic (MD) simulation further affirmed the findings and revealed that T124I induced conformational changes in the irisin domain of FNDC5, which may significantly affect its binding with protein FGF21, potentially impairing synergistic effects of FNDC5 and FGF21 on adipocyte browning and increasing risk for developing obesity and related disorders.**

Keywords FNDC5, In silico, Irisin, Obesity, SNPs

Obesity, a leading global nutritional disorder, is a major public health concern associated with diabetes mellitus, hypertension, insulin resistance, cardiovascular disease, and cancer, greatly impacting morbidity and mortality[1]. In this technologically advanced era, obesity is primarily driven by sedentary lifestyle and consumption of an unhealthy diet with high amounts of refined carbohydrates, along with genetic, endocrine, and environmental factors[2]. The global prevalence of this disorder has tripled from 1975 to 2016, affecting females more than males. In 2022, about 2.5 billion adults were overweight and almost 890 million had obesity[3]. Economic growth and urbanization have led to a substantial rise in obesity even in low- and middle-income countries, which was initially thought to be an issue of western world[2]. Considering its escalating prevalence and serious health risks, there is a dire need to identify the mechanisms and genetic predispositions underlying obesity.

Obesity is characterized by an imbalance between energy intake and energy utilization, leading to excessive accumulation of fats in adipose tissue[4]. Adipose tissue is of two types: white adipose tissue (WAT), which is involved in fat storage and brown adipose tissue (BAT), which is involved in energy burning. Browning is a

[1]Department of Biomedical Sciences, Dubai Medical College for Girls, Dubai, United Arab Emirates. [2]Department of Physiology, NUST School of Health Sciences, National University of Sciences and Technology, Islamabad 44000, Pakistan. [3]National University of Sciences and Technology, Islamabad 44000, Pakistan. [4]Department of Biosciences, COMSATS University, Islamabad 44000, Pakistan. [5]Department of Biological Sciences, National University of Medical Sciences, Islamabad 44000, Pakistan. [6]School of Biological Sciences, University of the Punjab, Lahore 05422, Pakistan. [7]These authors contributed equally to this work. ✉email: hira.moin@gmail.com; zoya11khalid@gmail.com

process by which white adipocytes acquire characteristics similar to those of brown adipocytes, primarily by developing beige or brite (brown-in-white) features, and it can be stimulated by physical exercise[5]. This effect can be attributed to the action of various myokines, among which fibronectin type-III domain-containing protein-5 (FNDC5) is noteworthy due to its potential role in modulation of metabolism and protection against obesity[6].

FNDC5 is a transmembrane protein which was initially discovered in 2002 by two independent research teams and was shown to be expressed in skeletal muscle, heart, and brain tissues[7,8]. A pivotal study in 2012 revealed that during exercise, the ectodomain of skeletal muscle FNDC5 is cleaved and secreted into the bloodstream as "irisin". Irisin was proposed to promote the browning of WAT, potentially accounting for some of the positive effects of exercise on energy expenditure[9]. The *FNDC5* locus comprises 6 exons and encodes a protein of 209 amino acids. The protein chain consists of a signal peptide consisting of 28 amino acids, a fibronectin type-III domain (FN-III) consisting of 93 amino acids, a linker consisting of 30 amino acids, a transmembrane segment consisting of 19 amino acids, and an intracellular portion consisting of 39 amino acids[10]. The FN-III domain, together with a 19 amino acid linker (from amino acid 29 to 140), is suggested to be enzymatically separated from FNDC5 and given the name irisin[9]. This 112 amino acid irisin has a molecular weight of 12 KDa[11,12]. It is produced during exercise by the action of peroxisome proliferator-activated receptor-γ co-activator-1α (PGC1α), resulting in up-regulation of *FNDC5* gene[13,14]. Subsequently, N-terminal signal sequence of FNDC5 protein is cleaved and secreted into the blood as irisin[10]. Irisin has a half-life of one hour. The structure consists of a continuous inter-subunit β-sheet dimer, which has an important role in the activation and signaling of receptors. Irisin functions as a molecular imitator of physical activity, with 72% of the overall irisin released from skeletal muscles[15,16]. The mitogen-activated protein kinase (MAPK) pathway is primarily responsible for the peptide's essential physiological activities[6].

Irisin primarily induces browning of WAT, promotes thermogenesis by enhancing uncoupling protein-1 (UCP1), improves insulin sensitivity, and increases the metabolism of lipids and glucose[1,17]. Irisin levels exhibit a reduction in individuals diagnosed with type-II diabetes, cardiovascular disease (CVD), and non-alcoholic fatty liver disease (NAFLD)[18,19]. Irisin levels are elevated in both obesity and the initial phases of myocardial infarction and are protective[20]. An experimental study on mice demonstrated that the introduction of recombinant irisin led to a reduction in body mass index (BMI), blood insulin, and luteinizing hormone levels[21]. These findings illustrate the protective effects of this myokine and its potential as a therapeutic agent.

In addition to irisin, fibroblast growth factor-21 (FGF21) is a crucial representative among all reported myokines closely associated with adipocyte browning. Both are up-regulated by physical exercise and potentially play a beneficial role in counteracting obesity and its related metabolic disturbances[22,23]. FGF21 is predominantly expressed in the liver, adipose tissues[24] and skeletal muscle[25]. Exercise is a critical stimulator for FGF21 expression and its release from skeletal muscle[26]. Similar to irisin, FGF21 induces the browning of WAT and promotes the overexpression of PGC1α[9,27].

In humans, single nucleotide polymorphisms (SNPs) represent the most common source of genetic variation[28]. The majority of metabolic diseases are linked to these SNPs[29,30]. Single nucleotide alterations occurring within the coding regions (exonic), referred to as non-synonymous SNPs (nsSNPs), exert a more substantial influence on the functional properties of the gene product[31,32]. Over 50% of the SNPs associated with genetic disorders are nsSNPs, also referred to as missense variants[32]. These nsSNPs can affect protein function by decreasing solubility or destabilizing the protein structure[33].

Several SNPs of *FNDC5*, such as (rs3480 and rs16835198), (rs3480A/G, rs1746661G/T, rs1298190A/G, rs726344A/G and rs1570569G/T), have been identified. These SNPs have been investigated for their correlation with various metabolic parameters such as dyslipidemias, insulin sensitivity, and obesity[30,34]. However, the results of these studies have shown varying/ inconsistent findings. Individuals with rs3480 GG genotype have a reduced likelihood of developing obesity and a lower body mass index[34]. The rs3480 in homozygous forms enhances the susceptibility towards type-II diabetic mellitus[30]. The presence of the rs1746661G allele is correlated with elevated triglyceride levels. The rs157069TT genotype is correlated with elevated fasting insulin and Homeostatic Model Assessment of Insulin Resistance (HOMA-IR). It is also associated with reduced levels of circulating irisin[34]. The research in this area is driven by the possible implications of SNP on the development of metabolic diseases, and could be of value in developing therapeutic approaches which in turn could lead to decreased morbidity and mortality rates as well as reduced healthcare expenditure[30,34]. Therefore, investigating the potential association between different SNPs, along with their phenotypic effects can provide valuable insights into the molecular mechanisms underlying many complex Mendelian diseases[33]. While experimental validation remains essential, computational methods for SNP screening are highly valuable for the identification and prioritization of candidate nsSNPs for detailed experimental analysis[35].

As the role of irisin is critical in obesity, the present study was designed to identify the candidate harmful/ high-risk nsSNPs of the *FNDC5* gene. The authors aimed to elucidate the relationship between these genetic polymorphisms and their possible phenotypic effects. The objective was pursued by using an in silico based combinatorial approach that integrated various bioinformatics tools. The identified nsSNPs are expected to cause functional and structural damage by decreasing the overall stability of the bound complex of irisin (secreted domain of FNDC5) with FGF21. This novel focus is the first to report the potential implications of nsSNPs on the FNDC5-FGF21 interaction that might contribute to the development of various metabolic disorders.

Results

Retrieval of sequence of FNDC5 protein

The protein sequence of FNDC5 was retrieved from the Uniprot database and the NCBI (National Centre for Bioinformatics Information) and further analyses were conducted.

Retrieval of missense SNPs of *FNDC5* gene

SNPs of the gene were retrieved from NCBI dbSNP as it is the most appropriate and widespread database. A total of 4734 SNPs of *FNDC5* were retrieved, out of which 172 were missense SNPs (supplementary Table 1), 83 were synonymous SNPs, 3124 intronic mutations, and the rest were other types of SNPs (Fig. 1).

Deleterious SNPs in *FNDC5* gene identified through various tools

All the variants in the172 nsSNPs were mapped to isoform 1 of *FNDC5*, reducing the total to 20 nsSNPs. These nsSNPs were then analyzed using five computational tools; SIFT (Sorting intolerant from tolerant)[36], PHD-SNP (Predictor of human deleterious single nucleotide polymorphism)[37], PROVEAN (Protein variation effect analyzer)[38], PANTHER (Protein analysis through evolutionary relationships)[39], and SNP&GO (Single Nucleotide Polymorphism & Gene Ontology)[40]. Each tool predicted a variant as either deleterious (damaging) or neutral. The final label was based on the majority voting among the five tools. We have considered those variants as deleterious which were predicted as damaging/deleterious by three out of five tools. The results indicate that a total of eight variants were predicted as damaging, including N39K, R78H, R209H, T124I, L150P, L156V, V83M, and T86I. Hence, these were further subjected to structure analysis.

The list of these nsSNPs are given in Table 1.

Structural and functional modifications of FNDC5 protein predicted by MutPred2

All the shortlisted nsSNPs of *FNDC5* were submitted to MutPred2 web server to predict alterations in structure and function of proteins[41]. For N39K, predictions included altered transmembrane protein ($p = 0.000063$), loss of loop ($p = 0.0052$), and loss of N-linked glycosylation at N39 ($p = 0.0095$). No altered molecular mechanism was predicted for R78H. For T124I, predicted changes comprised loss of intrinsic disorder ($p = 0.04$), loss of SUMOylation at K123 ($p = 0.04$) and altered transmembrane protein ($p = 0.02$). For L150P, predictions included gain of intrinsic disorder ($p = 0.02$), altered transmembrane protein ($p = 0.000073$), altered stability ($p = 0.008$), and gain of pyrrolidone carboxylic acid at Q148 ($p = 0.03$). No altered molecular mechanism was predicted for R209H. For variant T86I predictions comprised loss of N-link glycosylation ($p = 0.00019$), altered transmembrane protein ($p = 0.00033$), and loss of disulfide linkage at C90 ($p = 0.05$). For V83M, predictions of altered transmembrane protein ($p = 0.00094$), loss of N-linked glycosylation at N84 ($p = 0.001$), and altered stability ($p = 0.03$) were observed, and for L156V no alteration was predicted.

Stability modification prediction by I-MUTANT2.0

The stability of the variations that occurred was predicted by I-MUTANT 2.0[42]. The eight shortlisted high-risk SNPs of *FNDC5* were submitted to I-MUTANT 2.0 to calculate the reliability index and Gibbs free energy value. Results revealed that after mutation all the SNPs had a decrease in their stability and hence could cause damage to the protein. The details are given in Table 2.

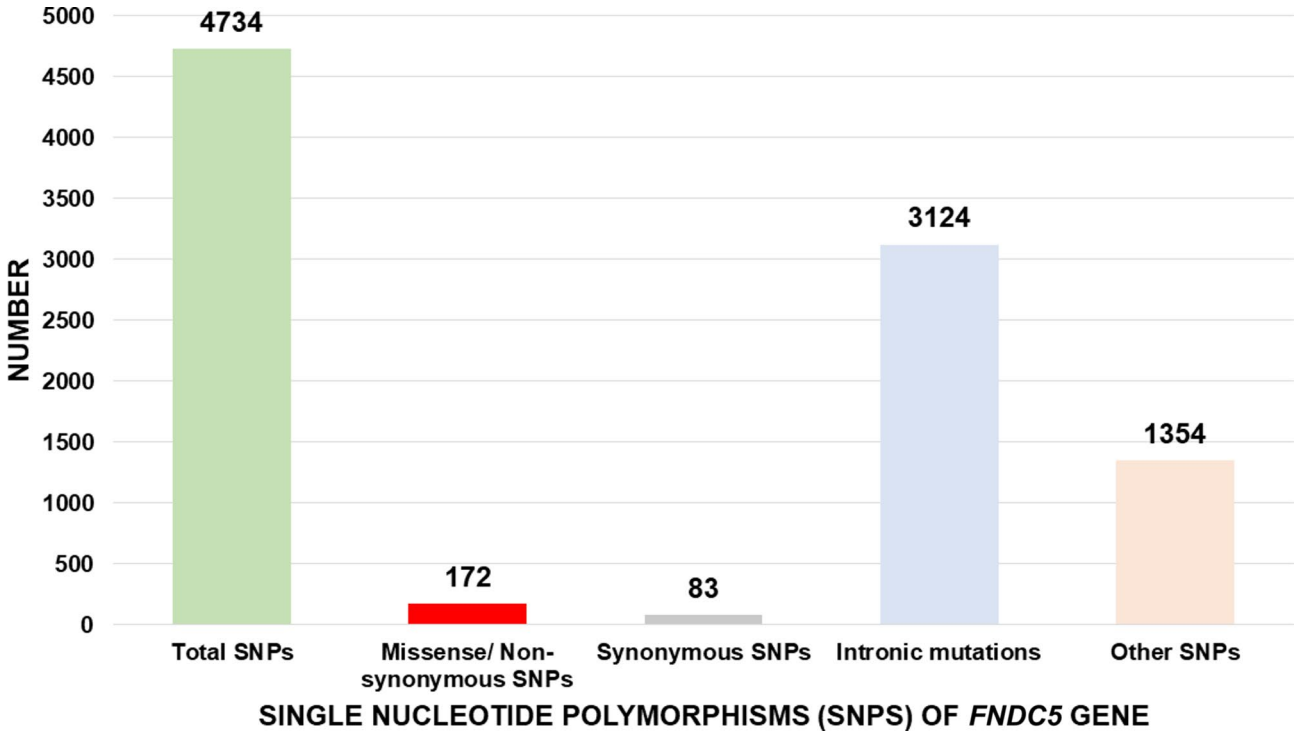

Fig. 1. Classification and frequency of various types of SNPs in the *FNDC5* gene according to NCBI dbSNP database. FNDC5 = fibronectin type-III domain-containing protein-5.

SNP ID	Amino acid exchange	MAF	REF allele	ALT allele	SIFT	PhD-SNP	PROVEAN	PANTHER	SNP&GO	Final label
rs200027292	I212T	G = 0.000135/6 (ALFA) G = 0.000072/18 (GnomAD_exomes) G = 0.000107/15 (GnomAD)	A	G	Deleterious (Low confidence)	Neutral	Neutral	Neutral	Neutral	Neutral
rs375151828	I80L	NA	T	G	Deleterious	Deleterious	Neutral	Neutral	Neutral	Neutral
rs368098828	K72E	C = 0.000071/1 (ALFA) C = 0.000004/1 (GnomAD_exomes) C = 0.000008/1 (ExAC) C = 0.000021/3 (GnomAD) C = 0.000023/6 (TOPMED) C = 0.000077/1 (GoESP)	T	C	Deleterious	Neutral	Neutral	Neutral	Neutral	Neutral
rs377741902	L150P	G = 0./0 (ALFA) G = 0.000004/1 (TOPMED) G = 0.000007/1 (GnomAD)	A	G	Deleterious	Deleterious	Deleterious	Deleterious	Deleterious	Deleterious
rs138727728	L156V	A = 0.001028/46 (ALFA) A = 0.00027/1 (TWINSUK) A = 0.000468/2 (1000Genomes)	A	A/C	Neutral	Deleterious	Neutral	Deleterious	Deleterious	Deleterious
rs370511876	L77P	G = 0.000043/1 (ALFA) G = 0.000004/1 (TOPMED) G = 0.000007/1 (GnomAD)	A	G	Neutral	Neutral	Neutral	Neutral	Neutral	Neutral
rs143697125	N185S	C = 0.000068/12 (ALFA) C = 0.000072/18 (GnomAD_exomes) C = 0.000099/12 (ExAC)	T	C	Neutral	Neutral	Neutral	Neutral	Neutral	Neutral
rs202111610	N187K	C = 0./0 (ALFA) C = 0.000007/1 (GnomAD)	G	C	Neutral	Neutral	Neutral	Neutral	Neutral	Neutral
rs55783359	N39K	A = 0./0 (ALFA) A = 0.000008/2 (TOPMED) A = 0.000014/2 (GnomAD)	G	A/T	Deleterious	Deleterious	Deleterious	Deleterious	Deleterious	Deleterious
rs370205345	Q148P	G = 0./0 (ALFA) G = 0.000028/7 (GnomAD_exomes) G = 0.000033/4 (ExAC)	T	C/G	Not found	Not found	Neutral	Not found	Not found	Neutral
rs369474610	R126H	T = 0./0 (ALFA) A = 0.000004/1 (GnomAD_exomes) T = 0.000021/3 (GnomAD)	C	A/T	Neutral	Neutral	Neutral	Deleterious	Neutral	Neutral
rs144593537	R209H	T = 0.000068/3 (ALFA) T = 0.000042/11 (TOPMED) T = 0.000064/16 (GnomAD_exomes)	C	T	Deleterious	Neutral	Deleterious	Deleterious	Neutral	Deleterious
rs373917435	R75Q	T = 0.000045/2 (ALFA) T = 0.00003/8 (TOPMED) T = 0.000036/5 (GnomAD)	C	T	Deleterious	Neutral	Neutral	Deleterious	Neutral	Neutral
rs140092865	R78H	T = 0.000045/2 (ALFA) T = 0.000008/1 (ExAC) T = 0.000024/6 (GnomAD_exomes)	C	A/T	Deleterious	Deleterious	Deleterious	Deleterious	Neutral	Deleterious
rs185141197	T124I	A = 0.000032/6 (ALFA) A = 0.000071/2 (TOMMO) A = 0.000354/43 (ExAC)	G	A/T	Deleterious	Neutral	Deleterious	Deleterious	Neutral	Deleterious
rs185141197	T199I	A = 0.000032/6 (ALFA) A = 0.000071/2 (TOMMO) A = 0.000354/43 (ExAC)	G	A/T	Deleterious	Neutral	Neutral	Neutral	Neutral	Neutral
rs374085063	T86I	A = 0./0 (ALFA) A = 0.000004/1 (GnomAD_exomes) A = 0.000014/2 (GnomAD)	G	A	Deleterious	Deleterious	Deleterious	Deleterious	Deleterious	Deleterious
rs189231805	V159I	T = 0.000079/14 (ALFA) T = 0.000036/5 (GnomAD) T = 0.000038/10 (TOPMED)	C	T	Neutral	Deleterious	Neutral	Neutral	Neutral	Neutral
rs200824057	V160M	T = 0.000043/1 (ALFA) T = 0.000007/1 (GnomAD) T = 0.000008/2 (TOPMED)	C	T	Deleterious	Not found	Neutral	Not found	Not found	Neutral
rs376090198	V83M	T = 0.000144/27 (ALFA) T = 0.000077/1 (GoESP) T = 0.000132/35 (TOPMED)	C	T	Deleterious	Deleterious	Deleterious	Deleterious	Neutral	Deleterious

Table 1. List of nsSNPs of *FNDC5* gene predicted as deleterious by various bioinformatics tools. The table presents the details of the short-listed nsSNPs of human *FNDC5* gene in coding sequence (CDS) region located on chromosome 1 (Build: GRCh37.74), identified using various bioinformatics tools: SIFT = sorting intolerant from tolerant), PHD-SNP = predictor of human deleterious single nucleotide polymorphism, PROVEAN = protein variation effect analyzer, PANTHER = protein analysis through evolutionary relationships, and SNP&GO = single nucleotide polymorphism & gene ontology. nsSNP = non-synonymous single nucleotide polymorphism, FNDC5 = fibronectin type-III domain-containing protein-5, MAF = mean allele frequency.

SNPs ID	Mutations	pH	Temp. (°C)	SVM2 prediction effect (stability)	ΔΔG value prediction (Kcal/mol.)	RI
rs55783359	N39K	7	25	Decrease	-1.65	9
rs140092865	R78H	7	25	Decrease	-1.31	8
rs144593537	R209H	7	25	Decrease	-2.11	8
rs185141197	T124I	7	25	Decrease	-1.03	4
rs377741902	L150P	7	25	Decrease	-3.01	6
rs138727728	L156V	8	25	Decrease	-0.81	7
rs376090198	V83M	7	25	Decrease	-1.71	7
rs374085063	T86I	7	25	Decrease	-093	7

Table 2. I-MUTANT 2.0 prediction results for deleterious nsSNPs of the *FNDC5* gene. SVM = support vector machine, ΔΔG = Gibbs free energy, RI = reliability index, FNDC5 = fibronectin type-III domain-containing protein-5.

SNPs ID	Mutations	Conservation score	Prediction
rs55783359	N39K	Exposed-functional	Highly conserved
rs140092865	R78H	Exposed-functional	Highly conserved
rs144593537	R209H	Exposed-functional	Highly conserved
rs185141197	T124I	Exposed-functional	Highly conserved
rs377741902	L150P	Buried	Conserved
rs138727728	L156V	Buried	Conserved
rs376090198	V83M	Buried-structural	Highly conserved
rs374085063	T86I	Exposed-functional	Highly conserved

Table 3. ConSurf prediction of phylogenetic conservation for deleterious nsSNPs in the *FNDC5* gene. FNDC5 = fibronectin type-III domain-containing protein-5.

Conservation profiling of the deleterious nsSNPs in *FNDC5* gene

Results from the web server ConSurf[43] revealed structural and functional importance and conservation levels of all the amino acid residues of FNDC5, but only high-risk nsSNPs were focused. The results are tabulated in Table 3 (color coding bar showing conservation score is provided in supplementary Fig. 1).

Analysis of protein-protein interaction using STRING

The STRING (Search Tool for the Retrieval of Interacting Genes/Proteins)[71] predicted physical interaction of FNDC5 with FGF21, UCP1, PPARGC1A (peroxisome proliferator-activated receptor-γ co-activator-1α; PGC1α), FN1 (fibronectin1), MSTN (myostatin), and METRN (meteorin) (Fig. 2). FGF21 showed the combined score of 0.77. Additionally, FGF21 and FNDC5 proteins are co-expressed. The putative homologs are also present in other organisms which makes FGF21 a string interacting candidate. Consequently, FGF21 was selected and docking analysis was conducted for these two proteins.

Molecular docking

The Cluspro web server was utilized to analyze the impact of mutations on the wild type complex and the mutant complexes[44]. From the above analyses we identified the eight variants that were negatively affecting the protein stability and were also conserved. These variants were further processed for docking analysis which can further reveal if the particular mutation is favoring this interaction of two proteins or halting it. We queried ClusPro for the wild-type complex of FNDC5-FGF21 and mutant complexes N39K-FGF21, R78H-FGF21, R209H-FGF21, T124I-FGF21, L150P-FGF21, L156V-FGF21, V83M-FGF21, and T86I-FGF21 in order to analyze the change in overall energy and stability of the interacting complex. The server generated a total of 9 clusters from which we selected cluster 1 as it showed the lowest binding energies which claims the stability of the complex. In order to identify the change in stability of the interacting complexes of wild-type and mutants we computed Buried Surface Area (BSA) using Python Molecular Graphics (PyMOL)[45]. Two of the variants T124I and L150P were predicted as candidate nsSNPs as the significant change in BSA was observed in these two variants. T124I was highly conserved and predicted as exposed and functional while L150P was predicted as buried in the core of the protein and conserved. The BSA measures the size of the interface in a protein-protein complex. The BSA of the wild-type complex was highest which showed that the complex is stable while the complex with T124I, L150P, showed the decrease in BSA which eventually means that the mutation is destabilizing the interacting proteins. BSA computes the size of the interacting proteins so, the larger the area the more stable the complex is. Moreover, in the rest of the variants N39K, R78H, R209H, L156V, V83M, and T86I, an increase in the BSA was observed which indicates that these variants might be positively affecting the interacting complex. The results are tabulated in Table 4. Also, we analyzed the change in hydrogen bonds using Python script with MDAnalysis[46] and the results are tabulated in Table 5. Higher number of hydrogen bonds indicated a stronger interaction

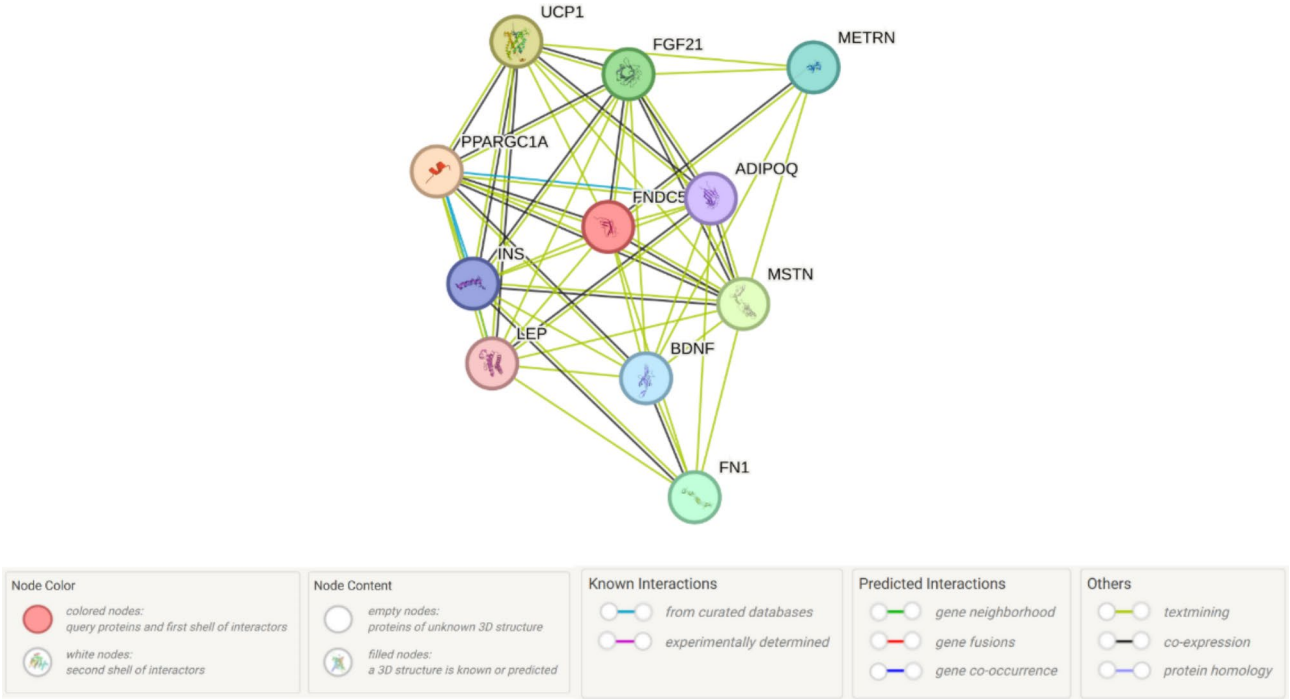

Fig. 2. Protein-protein interaction network of FNDC5 predicted by STRING, showing key interactions with FGF21, UCP1, PPARGC1A, FN1, MSTN, and METRN. FNDC5 = fibronectin type-III domain-containing protein-5, FGF21 = fibroblast growth factor21, UCP1 = Uncoupling protein1, PPARGC1A = peroxisome proliferator-activated receptor-γ co-activator-1α; PGC1α, FN1 = fibronectin1, MSTN = myostatin, METRN = meteorin.

Interacting complex	Buried surface area (BSA)
Wild-type	3358.145
N39K-FGF21	3356.12
R78H-FGF21	3738.23
R209H-FGF21	3634.67
T124I-FGF21	2789.816*
L150P-FGF21	2683.45*
L156V- FGF21	3560.347
V83M-FGF21	3601.62
T86I- FGF21	3827.900

Table 4. Buried surface area computed for the wild-type and mutant FNDC5-FGF21 interacting complexes using PyMOL. *BSA < < wild-type complex. FNDC5 = fibronectin type-III domain-containing protein-5, FGF21 = fibroblast growth factor21.

between the bound complexes. From the results it can be observed that the decrease in number of hydrogen bonds are observed which can eventually lead to the loss of stability of the protein complex due to mutation.

HOPE webserver

Two of the mutants, T124I-FGF21, and L150P-FGF21, predicted as high-risk variants, were further analyzed with HOPE (Have (y)Our Protein Explained) webserver[47]. In the mutant T124I the wild-type and mutant amino acids differed in size. The mutant residue was bigger than the wild-type residue. The wild-type residue was buried in the core of the protein. The mutant residue was bigger and probably would not fit. The hydrophobicity of the wild-type and mutant residue differed. The mutation would likely cause loss of hydrogen bonds in the core of the protein and as a result disturb correct folding. The mutated residue was located in a domain that is important for binding of other molecules. It is possible that the mutation could disturb these contacts. In the variant L150P, the wild-type and mutant amino acids differed in size. The mutant residue was smaller, that could lead to loss of interactions. This analysis further validated the predicted results.

Additionally, comparative analysis of wild-type and mutant FNDC5 proteins by was done using HOPE (predicted effects of mutants along with 3D structure are provided in supplementary Table 2).

Interacting complex	Hydrogen bond count
Wild-type	144
N39K-FGF21	98
R78H-FGF21	101
R209H-FGF21	99
T124I-FGF21	99
L150P-FGF21	99
L156V- FGF21	98
V83M-FGF21	101
T86I- FGF21	104

Table 5. Hydrogen-bond count computed for the wild-type and mutant FNDC5-FGF21 interacting complexes. FNDC5 = fibronectin type-III domain-containing protein-5, FGF21 = fibroblast growth factor21.

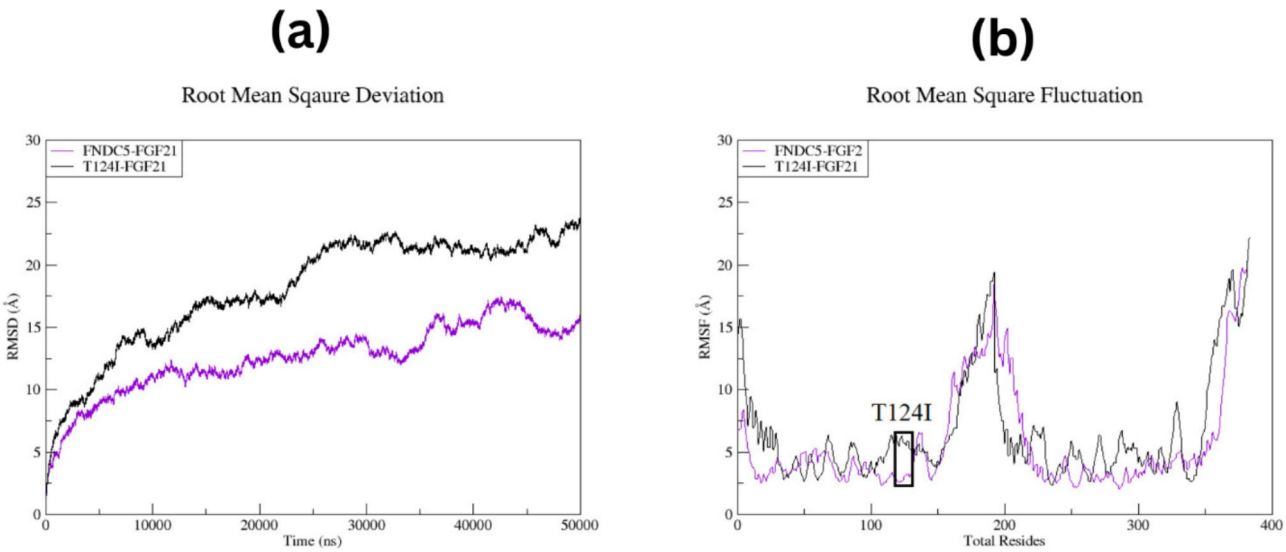

Fig. 3. (**a**) Root mean square deviation plots of the wild-type (FNDC5-FGF21) and mutant (T124I-FGF21) docked complexes. (**b**) Root mean square fluctuation plots of the wild-type (FNDC5-FGF21) and mutant (T124I-FGF21) docked complexes. FNDC5 = fibronectin type-III domain-containing protein-5, FGF21 = fibroblast growth factor21.

MD simulation

MD simulations of both the wild-type and mutant docked complexes were conducted using AMBER20 (Assisted Model Building with energy Refinement)[48]. The aim was to study how the highly conserved nsSNP, T124I, affects the dynamic behavior of FNDC5 and its interaction pattern with neighboring FGF21 protein. Important statistical analysis was performed on the trajectories of MD simulations to decipher the backbone stability and residual flexibility. The first stage was to compute the root mean square deviation (RMSD), which is used to identify the average distance between backbone carbon alpha atoms of overlay frames. The RMSD is a critical metric in the analysis of trajectory equilibration. Wild-type FNDC5-FGF21 protein and mutated T124I-FGF21 protein were plotted as a function of time to determine the stability of the backbone carbon alpha atoms. The findings show that wild-type FNDC5-FGF21, had a low RMSD (12.86 Å) value as compared to the mutated one. The RMSD plot for the mutated complex showed a trend of continuously increasing mean value (18.62 Å) due to the perturbations and conformation rearrangements to the structure introduced by the SNP (Fig. 3a). It further confirms the aforementioned findings and beliefs that a T124I mutation in *FNDC5* is responsible for this instability.

Afterward, the system trajectories were subjected to root mean square fluctuations (RMSF) to determine their stability. The RMSF values for the C atoms in each residue were calculated in order to identify the flexible regions and the amplitude of displacement of atoms in the residue (Fig. 3b). It was discovered that the average RMSF value for the Wild-type FNDC5-FGF21 system was 5.73 Å. Fluctuations in the graph indicate the flexibility of pocket residues in the molecule. The average RMSF value for the system in the instance of mutant T124I-FGF21 was 6.66Å. The RMSF for the majority of residues was lower than expected, suggesting that they moved less throughout the simulation. However, it was discovered that there was a variation at amino acid number 124, which is the amino acid at which the mutation happened. It may be deduced from this that mutation caused a conformational shift in structure, which in turn led to increased mobility, since high fluctuation is an indicator of

flexibility. The findings of MD simulation further confirmed that T124I mutation in *FNDC5* is likely responsible for a conformational change in irisin domain of FNDC5 protein and instability of the mutant complex, thereby affecting the interaction of FNDC5 with FGF21.

Discussion

Energy expenditure is instrumental in the prevention and amelioration of obesity and its associated metabolic disorders[49]. Current literature emphasizes the significant role of myokines as mediators of the beneficial effects of physical activity on metabolic health. Among these myokines, FNDC5 and its secreted product: irisin, have gained importance because of their potential role in browning of WAT. Hence, mutation of *FNDC5* gene may have deleterious impact on the functioning of this protein. Some SNPs in *FNDC5* have been studied in the context of various metabolic disorders, however, computational data analyzing these mutations remains limited. Therefore, identifying potential SNPs in the *FNDC5* is important to elucidate the role of FNDC5 and irisin in obesity and related disorders. In the present study, we performed computational analyses to predict high-risk SNPs of *FNDC5* and further assessed its variants that showed a significant decrease in protein stability by computing the buried surface area of the variants and the wild-type.

Circulating irisin is cleaved from the plasma membrane protein FNDC5 in response to exercise, with *FNDC5* gene predominantly expressed in skeletal muscles[9]. Irisin plays a critical role in metabolic regulation by promoting the browning of WAT. This browning process is characterized by the up-regulation of PGC1α and the UCP1, which subsequently enhances thermogenesis and energy expenditure[50,51]. Raschke et al. initially proposed that the human *FNDC5* gene has reduced translation efficiency, resulting in minimal irisin production and questioning its physiological role in humans[52]. However, recent studies report detectable levels of irisin linked to various metabolic functions, suggesting that *FNDC5* may indeed produce a fully functional protein, meriting further investigation[13,53].

The present study used various bioinformatics tools to identify and analyze the high-risk SNPs in *FNDC5* along with their structural and functional significance. nsSNPs were selected because these variants are commonly associated with disease pathogenesis due to their potential to alter protein function[54]. For *FNDC5*, The most deleterious variants predicted included N39K, R78H, R209H, T124I, L150P, L156V, V83M, and T86I. Further, the stability and conservation analyses categorized the variants as either conserved or variable and assessed their impact as favorable or unfavorable. Protein-protein interaction analysis predicted strong interaction between FNDC5 and FGF21. Moreover, the putative homologs are also present in other organisms, so the selected FNDC5 variants were docked with FGF21. Consequently, the docking protocol indicated that the contribution of each variant was either stabilizing or destabilizing the interaction of FNDC5 with FGF21. The computed BSA predicted T124I and L150P as candidate SNPs, because these variants showed a decrease in BSA, which is important to analyze the stability of the protein-protein interaction. The wild-type complex with the highest BSA, is expected to be more stable, as a larger, predominantly hydrophobic BSA tends to favor stable interactions by minimizing water exposure. The findings of MD simulation confirmed that T124I mutation in *FNDC5* is likely responsible for a conformational change in irisin domain of FNDC5 protein and instability of the mutant complex, thereby affecting the interaction of FNDC5 with FGF21.

FGF21 and irisin may act synergistically to promote the browning of white adipocytes[55]. Studies have also shown that obesity is associated with reduced circulating and adipose tissue expression levels of FGF21 and irisin, along with decreased expression of their specific receptors: β-Klotho and fibroblast growth factor receptor-1 (FGFR1) for FGF21, and integrin subunit alpha-5 (ITGA5) for irisin[56–60]. de la Torre-Saldaña VA. et al.. explored the association between serum levels of FGF21 and irisin after exercise and reported that despite increases in both FGF21 and irisin following exercise, the correlation between their levels post-exercise was not significant, indicating independent regulation for each myokine[49].

Zhu et al. employed the CRISPRa (Clustered Regularly Interspaced Short Palindromic Repeats-dead Cas9) system to induce the expression of the myokines FGF21 and FNDC5 in mouse C2C12 myoblast cells. Their findings demonstrated that the co-activation of *FGF21* and *FNDC5* resulted in higher efficiency at both mRNA and protein levels compared to the activation of a single myokine. They posited that this outcome might be attributable to the synergistic effects of FGF21 and irisin on muscle cell function. However, this synergistic effect was not replicated in vivo. In diet-induced obese C57BL/6J mice, despite the activation of both *FGF21* and *FNDC5*, no significant improvement was observed compared to mice treated with AAVs (Adeno-associated virus) targeting a single myokine[61].

FGF21 and irisin are among the key myokines recognized as crucial mediators of the beneficial effects of exercise on metabolism. Consequently, they represent potential targets for the development of novel therapeutic approaches to combat obesity and related metabolic disorders[55]. As such, elucidating the mechanisms through which these myokines operate and interact with each other unveils novel avenues for addressing metabolic health issues.

Although both exercise-induced myokines, FGF21 and irisin, stimulate browning of WAT through pathways involving increased expression of PGC1α, their mutual interaction remains less thoroughly understood. The present study revealed that the potentially deleterious and highly conserved nsSNPS of *FNDC5* were destabilizing and negatively affecting its interaction with *FGF21*. The identified polymorphisms, T124I and L150P, might potentially affect the irisin domain of FNDC5, the domain that is subsequently cleaved and secreted to induce the browning of WAT. Therefore, we hypothesize that these polymorphisms may impair the synergistic effects of FNDC5 and FGF21 on adipocyte browning, potentially increasing the risk for developing obesity and related disorders. While this study provides valuable predictions using in silico tools, these tools rely on computational algorithms and databases that may not reflect the full complexity of biological systems. In silico predictions, though informative, may have limitations in accuracy and specificity. Further studies and

experimental validations, including wet lab investigations, are necessary to confirm the effects of *FNDC5* SNPs on the functionality of the protein and their role in disease susceptibility.

Conclusion

The findings of this computational study revealed that two nsSNPs of *FNDC5*, T124I and L150P, by affecting the irisin domain, potentially impair the synergistic effects of FNDC5 and FGF21 on adipocyte browning, hence increasing the risk for developing obesity and related disorders. Experimental validation of these nsSNPs on *FNDC5* expression and stability, along with population-based clinical studies, could confirm these in silico findings and establish variant-disease correlations.

Methods

Identification of functional SNPs of *FNDC5*

The protein sequence of FNDC5 was queried from the Uniprot database, using an identifier "Q8NAU1-FNDC5-Human". The sequence comprises 212 amino acids. Afterwards, comprehensive data regarding all SNPs associated with the *FNDC5* gene were retrieved from NCBI SNP database (https://www.ncbi.nlm.nih.gov/snp/) on April 08, 2024. Following that, all the nsSNPs of the gene were identified and their relevant information, including accession numbers, positions, and amino acid change, were retrieved for further computational analyses.

Identification of the high-risk nsSNPs

For the comprehensive prediction of the functional impact of nsSNPs, five different tools were used, including SIFT, PROVEAN, PhD-SNP, PANTHER, and SNP&GO. Only those nsSNPs were considered for further analyses, which were predicted to be deleterious or damaging by three out of five tools. The details of the tools are discussed below.

SIFT

SIFT is a bioinformatics tool that predicts whether amino acid change has any impact on function and physical properties of protein[36]. Query sequence is submitted to the tool and nsSNPs are sorted out as tolerant or intolerant. Firstly, this tool searches for sequences that have similarity with query sequence and identifies those that have similar functions. Secondly, it procures alignments and calculates the possible tolerance index (TI) of all the SNPs. The threshold value of TI is 0.05. If the TI is less than 0.05, the SNP is considered to be deleterious or intolerant, and if the TI is equal or greater than 0.05, it is considered to be tolerant or non-pathogenic. Lower the TI, greater will be the possibility of SNP to be deleterious and vice versa[62]. rsIDs of the nsSNPs of FNDC5 were submitted to the SIFT tool (https://sift.bii.a-star.edu.sg/www/SIFT_dbSNP.html) and the analysis was done using default parameter settings[63]. The nsSNPs were sorted out as tolerant or intolerant.

PhD-SNP

This bioinformatics tool uses support vector machine (SVM) method and predicts whether the SNPs are neutral or diseased. The tool operates using three methods: hybrid, sequence-based, and sequence and profile-based methods[37]. The sequence of FNDC5 was submitted to PhD-SNP (https://snps.biofold.org/phd-snp/phd-snp.html). The position of mutations and new variants were submitted individually. All the other parameters were set to their default values.

PROVEAN

PROVEAN (http://provean.jcvi.org/seq_submit.php) is a bioinformatics database which provides information regarding the potential impact of any amino acid substitution on biological function of protein. The database provides results in a tabulated format: if the value ranges from 0.0 to 0.5, it indicates the variant is deleterious, while if the value ranges from 0.5 to 1.0, it indicates the variant is tolerated[38]. The raw sequence of the protein FNDC5 was submitted to this server to predict the impact of variants on biological function.

PANTHER

PANTHER is a tool that provides functional predictions of nsSNP affecting the protein. It estimates the duration for which an amino acid has been conserved in evolutionary pathway leading to the protein of interest, using a method known as PANTHER-PSEP (position-specific evolutionary preservation)[39]. The longer the duration, the greater will be the functional impact of nsSNP on the protein[64]. PANTHER categorizes the SNPs as possibly benign, possibly damaging, and probably damaging, based on the p-del score. SNPs with p-del score of 0.5, less than 0.5, and greater than 0.5 are considered possibly damaging, possibly benign, and probably damaging, respectively[65]. Protein sequence for FNDC5, along with the substitutions was submitted to PANTHER and default settings were used for other parameters.

SNP & GO

SNP & GO is a bioinformatics tool that predicts disease associated variations by using gene ontology terms[40]. It can predict using three types of inputs: raw sequence, sequence file, or Swiss-Prot code. If the probability of the variation is greater than 0.5, it is classified as diseased SNP and if less than 0.5, it is considered neutral[66]. The raw sequence of the protein FNDC5 was submitted to this server (https://snps.biofold.org/snps-and-go/snps-and-go.html), along with the mutations.

Identification of structural and functional properties of SNPs by MutPred2

MutPred2 (http://mutpred.mutdb.org/) is a web-based tool that effectively distinguishes between the diseased or benign amino acid substitutions. It identifies the potential impact of these substitutions on over 50 various

protein properties, thereby enabling the inference of the molecular mechanism of the pathogenicity[41]. This web server provides results based on SIFT and 14 different functional and structural properties, such as gain of intrinsic disorders, gain of B-factor, loss of phosphorylation, gain of catalytic site, altered metal binding, and transmembrane protein[67]. This server takes benign polymorphism from SWISS-PROT and deleterious from human gene mutation database. The FASTA sequence of the FNDC5 protein was submitted to the MutPred2 web server along with specific substitutions. The threshold was set at 0.05. The tool classified the substitutions as either neutral or deleterious and provided their structural and functional impacts. A p-value less than 0.05 indicated a confident prediction, while a p-value less than 0.01 indicated very high confidence in the pathogenicity of the substitution.

Analysis of FNDC5 protein stability by I-MUTANT 2.0

I-MUTANT 2.0 is a software that works on SVM based algorithms (http://gpcr2.biocomp.unibo.it/cgi/predictors/I-Mutant3.0/I-Mutant3.0.cgi).[43] This tool is used to predict the stability of proteins when mutations occur in them[68]. The change in the Gibbs free energies (ΔΔG) of the wild-type and mutants can predict the change in the stability of the protein structure. I-MUTANT 2.0 provides data from ProTherm as well, which is an experimental data library on protein mutations. If the ΔΔG is from −0.5 kcal/mol to ≤0.5 kcal/mol, it is considered neutral. If energy is greater than 0.5 kcal/mol, the protein structure is considered largely stable, and if the energy is less than −0.5, it is considered unstable[69]. Additionally, I-MUTANT 2.0 provides a reliability index, ranging from 1 to 10. Reliability index closer to 10 signifies that the outcome is more reliable. All the SNPs of *FNDC5* were submitted keeping the default setting for parameters i.e., pH of 7.0 and temperature of 25 °C.

Evaluation of evolutionary conservation of the FNDC5 protein by ConSurf

ConSurf (https://consurf.tau.ac.il/consurf_index.php) is a bioinformatics tool that was used to estimate and analyze the conservation profile of amino acid or nucleotide positions in a protein or nucleic acid sequence[43]. Analysis through this tool was performed to identify phylogenetic relations among homologous sequences. Multiple sequences were aligned using the MUSCLE (Multiple Sequence Comparison by Log-Expectation) tool. This tool was preferred because of its accuracy in computing evolutionary rate, based on the methods it utilizes i.e., Bayesian and maximum likelihood methods[70]. The results obtained from this tool are interpreted based on conservation score, ranging from 1 to 9, which provides information regarding the structural and functional characteristics of the protein (i.e., whether the proteins were exposed or buried or if they were structurally or functionally important). The score determines residue wise conservation of the protein which ranges from 1 to 9. Number 9 being the highest score depicts that the residue is highly conserved while number 1 predicts that the amino acid is less conserved.

Analysis of interaction of FNDC5 with other proteins

A protein interacts with many other proteins inside the cell and this interaction is important for the function and regulation of protein. The functional interaction of FNDC5 with other proteins inside the cells was predicted using STRING[71]. This tool uses its database of 24,584,628 proteins from 5,090 organisms and predicts protein–protein interaction networks either through direct or indirect association among proteins. The terms FNDC5 and *Homo sapiens* were searched as input options for STRING. This database identified various proteins that can interact with FNDC5. Out of all interacting proteins, we have selected FGF21, for which reported combined score was 0.77, both these proteins were also co-expressing with each other. In addition to that the putative homologs are also present in other organisms which makes FGF21 a string interacting candidate. Hence, we selected FGF21 and the two proteins were docked using the ClusPro web server[44] using the default settings in order to analyze the complex and the effect of mutations on it. The ClusPro predicts 10 different docked poses with different binding energies sorted by the scores. The score determines the stability of each docked complex. The ClusPro webserver follows the protocol of direct docking method that tends to perform rigid body docking by checking millions of conformations with the help of RMSD. On the basis of RMSD, the models were divided into clusters, each representing the probable model of the protein-protein-complex, sorted by the lowest energy models. These were further modified by energy minimization algorithms. To analyze the effect of mutations on the protein-protein interactions, buried surface area was calculated using PyMOL[45].

Protein structure analysis using HOPE webserver

The HOPE webserver is an automated program that analyzes the impact of mutations on the structure and function of the protein. It takes protein sequence as an input and identifies the effect of variants on the structure and function of the protein. This web server uses the 3D structure of the protein to identify the pathogenicity of each variant. Two of the mutants, T124I-FGF21, and L150P-FGF21, predicted as high-risk variants, were further analyzed with HOPE webserver[47].

Molecular dynamics simulations

To investigate the influence of the most detrimental SNP, T124I, in the structural and functional stability of the FNDC5, we ran MD simulation for 50 ns for both wild-type and mutant docked complex using AMBER20[48]. The solvation of the system was carried out in a TIP3P (transferable intermolecular potential 3-point) solvation box. The ff14SB force field was subsequently included to figure out the intermolecular and intra-molecular interactions using the Amber's Leap module. To neutralize the charges, sodium ions were introduced into the systems. Specifically, energy optimization was accomplished through 2000 steps of hydrogen atom minimization, 1000 steps of system solvation box energy minimization with a restraint of 200 kcal/mol^{-2} applied to the rest of the system, 1000 steps of the entire set of system atoms minimization with a restraint of 5 kcal/mol^{-2} applied to the system carbon alpha atoms, and 300 steps of non-heavy atom minimization with a restriction of 100 kcal

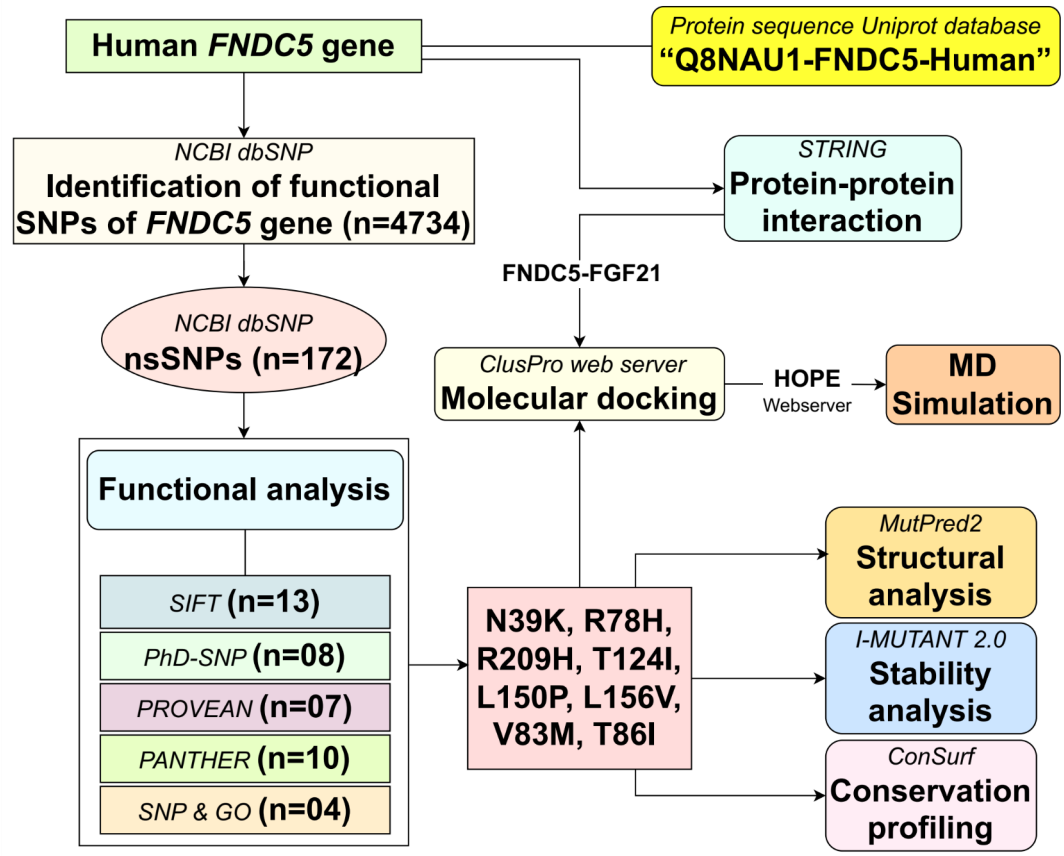

Fig. 4. Methodology of the study. FNDC5 = Fibronectin type-III domain-containing protein-5, FGF21 = fibroblast growth factor21, SIFT = sorting intolerant from tolerant, PROVEAN = protein variation effect analyzer, PHD-SNP = predictor of human deleterious single nucleotide polymorphism, SNP&GO = Single nucleotide polymorphism & gene ontology, PANTHER = protein analysis through evolutionary relationships), STRING = search tool for the retrieval of interacting genes/ proteins, HOPE = have (y)Our protein evaluated, nsSNP = non-synonymous SNP, MD = molecular dynamic.

In order to restrict hydrogen bond formation, the system was heated to 300 K using the NVT ensemble, which was assisted by Langevin dynamics and the SHAKE algorithm. We were able to achieve equilibration for 100 ps while maintaining pressure on the system using an NPT ensemble, which allowed us to constrain the C-atoms by 5 kcal/mol^{-2}. -ns trajectories were built during the third phase of the project. Non-bounded interactions were separated by a threshold distance of 8.0, which was added recently. The stability of the system was investigated by the use of the QtGrace program (https://sourceforge.net/projects/QtGrace), which performed an analytical calculation of structural parameters. The methodology is summarized in Fig. 4. Also, change in hydrogen bonds was analyzed using Python script with MDAnalysis[46].

Data availability

The datasets generated during and/or analyzed during the current study are available from the corresponding author on reasonable request.

Received: 8 August 2024; Accepted: 12 December 2024
Published online: 05 March 2025

References

1. Li, H. et al. The effect of irisin as a metabolic regulator and its therapeutic potential for obesity. *Int. J. Endocrinol.* **2021**(1), 6572342. https://doi.org/10.1155/2021/6572342 (2021).
2. Boutari, C. & Mantzoros, C. S. A 2022 update on the epidemiology of obesity and a call to action: as its twin COVID-19 pandemic appears to be receding, the obesity and dysmetabolism pandemic continues to rage on. *Metabolism* **133**, 155217. (2022).
3. World Health Organization. *Obesity and overweight.* (2021). https://www.who.int/news-room/fact-sheets/detail/obesity-and-overweight
4. Petridou, A., Siopi, A. & Mougios, V. Exercise in the management of obesity. *Metabolism* **92**, 163–169. https://doi.org/10.1016/j.metabol.2018.10.009 (2019).
5. Rashid, F. A., Abbas, H. J., Naser, N. A. & Addai Ali, H. A. Effect of long-term moderate physical exercise on Irisin between normal weight and obese men. *Sci. World J.* **2020**(1), 1897027 (2020).

6. Rabiee, F. et al. New insights into the cellular activities of Fndc5/Irisin and its signaling pathways. *Cell. Biosci.* **10**, 1–0. https://doi.org/10.1186/s13578-020-00413-3 (2020).
7. Ferrer-Martínez, A., Ruiz-Lozano, P. & Chien, K. R. Mouse PeP: A novel peroxisomal protein linked to myoblast differentiation and development. *Dev. Dyn.* **224**(2), 154–167. https://doi.org/10.1002/dvdy.10099 (2002).
8. Teufel, A., Malik, N., Mukhopadhyay, M. & Westphal, H. Frcp1 and Frcp2, two novel fibronectin type III repeat containing genes. *Gene* **297**(1–2), 79–83. https://doi.org/10.1016/s0378-1119(02)00828-4 (2002).
9. Boström, P. et al. A PGC1-α-dependent myokine that drives brown-fat-like development of white fat and thermogenesis. *Nature* **481**(7382), 463–468. https://doi.org/10.1038/nature10777 (2012).
10. Schumacher, M. A., Chinnam, N., Ohashi, T., Shah, R. S. & Erickson, H. P. The structure of irisin reveals a novel intersubunit β-sheet fibronectin type III (FNIII) dimer: Implications for receptor activation. *J. Biol. Chem.* **288**(47), 33738–33744. https://doi.org/10.1074/jbc.m113.516641 (2013).
11. Perakakis, N. et al. Physiology and role of irisin in glucose homeostasis. *Nat. Rev. Endocrinol.* **13**(6), 324–327. (2017).
12. Arhire, L. I., Mihalache, L. & Covasa, M. Irisin: A hope in understanding and managing obesity and metabolic syndrome. *Front. Endocrinol.* **10**, 524. https://doi.org/10.3389/fendo.2019.00524 (2019).
13. Maak, S., Norheim, F., Drevon, C. A. & Erickson, H. P. Progress and challenges in the biology of FNDC5 and irisin. *Endocr. Rev.* **42**(4), 436–456. https://doi.org/10.1210/endrev/bnab003 (2021).
14. Leustean, L. et al. Role of Irisin in endocrine and metabolic disorders—possible new therapeutic agent? *Appl. Sci.* **11**(12), 5579. https://doi.org/10.3390/app11125579 (2021).
15. Liu, C., Wei, A. & Wang, T. Irisin, an effective treatment for cardiovascular diseases? *J. Cardiovasc. Dev. Disease* **9**(9), 305. https://doi.org/10.3390/jcdd9090305 (2022).
16. Waseem, R. et al. FNDC5/irisin: Physiology and pathophysiology. *Molecules* **27**(3), 1118. https://doi.org/10.3390/molecules27031118 (2022).
17. Pinho-Jr, J. D. et al. Irisin and cardiometabolic disorders in obesity: A systematic review. *Int J Inflamm.* **2023**(1), 5810157. https://doi.org/10.1155/2023/5810157 (2023).
18. Polyzos, S. A. et al. Irisin in metabolic diseases. *Endocrine* **59**, 260–274. https://doi.org/10.1007/s12020-017-1476-1 (2018).
19. Zhang, R. et al. Association of circulating irisin levels with adiposity and glucose metabolic profiles in a middle-aged Chinese population: A cross-sectional study. *Diabetes Metab. Syndr. Obes.* **2020**, 4105–4112. https://doi.org/10.2147/DMSO.S275878 (2020).
20. Ho, M. Y. & Wang, C. Y. Role of irisin in myocardial infarction, heart failure, and cardiac hypertrophy. *Cells* **10**(8), 2103. https://doi.org/10.3390/cells10082103 (2021).
21. Majeed, S. et al. Effects of recombinant irisin on body mass index, serum insulin, luteinizing hormone and testosterone levels in obese female BALB/c mice. *J. Coll. Physicians Surg. Pak* **29**(8), 736–740 (2019).
22. Rodriguez, A., Becerril, S., Ezquerro, S., Mendez-Gimenez, L. & Fruhbeck, G. Crosstalk between adipokines and myokines in fat browning. *Rev. Acta Physiol.* **219**(2), 362–381. https://doi.org/10.1111/apha.12686 (2017).
23. Xie, T. & Leung, P. S. Roles of FGF21 and irisin in obesity-related diabetes and pancreatic diseases. *J. Pancreatol.* **3**(1), 29–34. https://doi.org/10.1097/JP9.0000000000000039 (2020).
24. Hondares, E. et al. Thermogenic activation induces FGF21 expression and release in brown adipose tissue. *J. Biol. Chem.* **286**, 12983–12990. https://doi.org/10.1074/jbc.m110.215889 (2011).
25. Izumiya, Y. et al. FGF21 is an Akt-regulated myokine. *FEBS Lett.* **582**, 3805–3810. https://doi.org/10.1016/j.febslet.2008.10.021 (2008).
26. Pedersen, B. K. & Febbraio, M. A. Muscles, exercise and obesity: skeletal muscle as a secretory organ. *Nat. Rev. Endocrinol.* **8**, 457–465. https://doi.org/10.1038/nrendo.2012.49 (2012).
27. Cuevas-Ramos, D. & Aguilar-Salinas, C. A. Modulation of energy balance by fibroblast growth factor 21. *Horm. Mol. Biol. Clin. Investig.* **30**(1), 20160023. https://doi.org/10.1515/hmbci-2016-0023 (2016).
28. Dabhi, B. & Mistry, K. N. In silico analysis of single nucleotide polymorphism (SNP) in human TNF-α gene. *Meta Gene* **2**, 586–595. https://doi.org/10.1016/j.mgene.2014.07.005 (2014).
29. Khalid, Z. & Almaghrabi, O. Mutational analysis on predicting the impact of high-risk SNPs in human secretary phospholipase A2 receptor (PLA2R1). *Sci. Rep.* **10**(1), 11750. https://doi.org/10.1038/s41598-020-68696-7 (2020).
30. Yang, X., Ni, L., Sun, J., Yuan, X. & Li, D. Associations between rs3480 and rs16835198 gene polymorphisms of FNDC5 with type 2 diabetes mellitus susceptibility: A meta-analysis. *Front. Endocrinol.* **13**, 946982. https://doi.org/10.3389/fendo.2022.946982 (2022).
31. Carninci, P. et al. The transcriptional landscape of the mammalian genome. *Science* **309**, 1559–1563. https://doi.org/10.1126/science.1112014 (2005).
32. Datta, A., Mazumder, M. H., Chowdhury, A. S. & Hasan, M. A. Functional and structural consequences of damaging single nucleotide polymorphisms in human prostate cancer predisposition gene RNASEL. *BioMed. Res. Int.* **2015**, 271458. https://doi.org/10.1155/2015/271458 (2015).
33. Mia, M. A., Uddin, M. N., Akter, Y. & Jesmin, Wal Marzan, L. Exploring the structural and functional effects of nonsynonymous SNPs in the human serotonin transporter gene through in silico approaches. *Bioinform. Biol. Insights* **16** https://doi.org/10.1177/11779322221104308 (2022).
34. Al-Daghri, N. M. et al. SNPs in FNDC5 (irisin) are associated with obesity and modulation of glucose and lipid metabolism in Saudi subjects. *Lipids Health Dis.* **15**, 1–8. https://doi.org/10.1186/s12944-016-0224-5 (2016).
35. Dash, R. et al. Computational SNP analysis and molecular simulation revealed the most deleterious missense variants in the NBD1 domain of human ABCA1 transporter. *Int. J. Mol. Sci.* **21**(20), 7606. https://doi.org/10.3390/ijms21207606 (2020).
36. Joshi, J. S. et al. Identifying the impact of structurally and functionally high-risk nonsynonymous SNPs on human patched protein using in-silico approach. *Gene Rep.* **23**, 101097. https://doi.org/10.1016/j.genrep.2021.101097 (2021).
37. Wang, M., Sun, Z., Akutsu, T. & Song, J. Recent advances in predicting functional impact of single amino acid polymorphisms: A review of useful features, computational methods and available tools. *Curr. Bioinform.* **8**(2), 161–176 (2013).
38. Choi, Y. & Chan, A. P. PROVEAN web server: a tool to predict the functional effect of amino acid substitutions and indels. *Bioinformatics* **31**(16), 2745–2747. https://doi.org/10.1093/bioinformatics/btv195 (2015).
39. Mishra, C., Kumar, S. & Yathish, H. M. Predicting the effect of non synonymous SNPs in bovine TLR4 gene. *Gene Rep.* **6**, 32–35. https://doi.org/10.1016/j.genrep.2016.11.005 (2017).
40. Mah, J. T., Low, E. S. & Lee, E. In silico SNP analysis and bioinformatics tools: A review of the state of the art to aid drug discovery. *Drug Discov. Today* **16**(17–18), 800–809. https://doi.org/10.1016/j.drudis.2011.07.005 (2011).
41. Laskar, F. S. et al. An in silico approach towards finding the cancer-causing mutations in human MET gene. *Int J Genomics* **2023**(1), 9705159. https://doi.org/10.1155/2023/9705159 (2023).
42. Singh, A., Singh, S. & Anbarasu, A. In silico evaluation of non-synonymous SNPs in IRS-1 gene associated with type II diabetes mellitus. *Res. J. Pharm. Tech.* **11**(5), 1957–1961. https://doi.org/10.5958/0974-360X.2018.00363.3 (2018).
43. Waheed, S. et al. Identification and in-silico study of non-synonymous functional SNPs in the human SCN9A gene. *Plos One* **19**(2), e0297367. https://doi.org/10.1371/journal.pone.0297367 (2024).
44. Kozakov, D. et al. The ClusPro web server for protein–protein docking. *Nat. Protoc.* **12**(2), 255–278. https://doi.org/10.1038/nprot.2016.169 (2017).
45. Schrodinger, L. L. C. The PyMOL molecular graphics system. *Version* **1**, 8 (2015).

46. Gowers, R. J. et al. *MDAnalysis: A Python package for the rapid analysis of molecular dynamics simulations* (Los Alamos National Laboratory (LANL), Los Alamos, NM (United States), 2019).
47. Venselaar, H., Te Beek, T. A., Kuipers, R. K., Hekkelman, M. L. & Vriend, G. Protein structure analysis of mutations causing inheritable diseases. An e-Science approach with life scientist friendly interfaces. *BMC Bioinform.* **11**, 1–0. https://doi.org/10.1186/1471-2105-11-548 (2010).
48. Case, D. et al. AMBER 22 (University of California, San Francisco, 2022).
49. de la Torre-Saldaña, V. A. et al. Fasting insulin and alanine amino transferase, but not FGF21, were independent parameters related with irisin increment after intensive aerobic exercising. *Rev. Invest. Clín.* **71**(2), 133–140. https://doi.org/10.24875/ric.18002764 (2019).
50. Kelly, D. P. Medicine. Irisin, light my fire. *Science* **336**, 42–43. https://doi.org/10.1126/science.1221688 (2012).
51. Lee, H. J. et al. Irisin, a novel myokine, regulates glucose uptake in skeletal muscle cells via AMPK. *Mol. Endocrinol.* **29**(6), 873–881. https://doi.org/10.1210/me.2014-1353. (2015)
52. Raschke, S. et al. Evidence against a beneficial effect of irisin in humans. *PloS one* **8**(9), e73680. https://doi.org/10.1371/journal.pone.0073680 (2013).
53. Albrecht, E. et al. Irisin–a myth rather than an exercise-inducible myokine. *Sci. Rep.* **5**(1), 8889. https://doi.org/10.1038/srep08889 (2015).
54. Ferrer-Costa, C., Orozco, M. & de la Cruz, X. Characterization of disease-associated single amino acid polymorphisms in terms of sequence and structure properties. *J. Mol. Biol.* **315**, 771–786. https://doi.org/10.1006/jmbi.2001.5255 (2002).
55. Lee, P. et al. Irisin and FGF21 are cold-induced endocrine activators of brown fat function in humans. *Cell. Metab.* **19**(2), 302–309. https://doi.org/10.1016/j.cmet.2013.12.017 (2014).
56. Diaz-Delfin, J. et al. TNF-alpha represses beta-Klotho expression and impairs FGF21 action in adipose cells: Involvement of JNK1 in the FGF21 pathway. *Endocrinology* **153**(9), 4238–4245. https://doi.org/10.1210/en.2012-1193 (2012).
57. Moreno-Navarrete, J. M. et al. Irisin is expressed and produced by human muscle and adipose tissue in association with obesity and insulin resistance. *J. Clin. Endocrinol. Metab.* **98**(4), E769–E778. https://doi.org/10.1210/jc.2012-2749 (2013).
58. Baruch, A. et al. Antibody-mediated activation of the FGFR1/Klothoβ complex corrects metabolic dysfunction and alters food preference in obese humans. *Proc. Natl. Acad. Sci. USA.* **117**(46), 28992–29000. https://doi.org/10.1073/pnas.2012073117 (2020).
59. Moure, R. et al. Levels of β-klotho determine the thermogenic responsiveness of adipose tissues: Involvement of the autocrine action of FGF21. *Am. J. Physiol. Endocrinol. Metab.* **320**(4), E822–E834. https://doi.org/10.1152/ajpendo.00270.2020 (2021).
60. Fu, T. et al. Integrin αV mediates the effects of irisin on human mature adipocytes. *Obes. Facts* **15**(3), 442–450. https://doi.org/10.1159/000523871 (2022).
61. Zhu, H. et al. CRISPRa-based activation of Fgf21 and Fndc5 ameliorates obesity by promoting adipocytes browning. *Clin. Transl Med.* **13**(7), e1326. https://doi.org/10.1002/ctm2.1326 (2023).
62. Subbiah, H. V., Babu, P. R. & Subbiah, U. Determination of deleterious single-nucleotide polymorphisms of human LYZ C gene: An in silico study. *J. Genet. Eng. Biotechnol.* **20**(1), 92. https://doi.org/10.1186/s43141-022-00383-8 (2022).
63. Matsubara, A. et al. Isolation and characterization of the human AKT1 gene, identification of 13 single nucleotide polymorphisms (SNPs), and their lack of association with type II diabetes. *Diabetologia* **44**(3), 910. https://doi.org/10.1007/s001250100577 (2001).
64. Tang, H. & Thomas, P. D. Tools for predicting the functional impact of nonsynonymous genetic variation. *Genetics* **203**(2), 635–647. https://doi.org/10.1534/genetics.116.190033 (2016).
65. Mi, H. et al. PANTHER version 11: Expanded annotation data from gene ontology and reactome pathways, and data analysis tool enhancements. *Nucleic Acids Res.* **45**(D1), D183–D189. https://doi.org/10.1093/nar/gkw1138 (2017).
66. Siddiqua, H. et al. SHANK3 genetic polymorphism and susceptibility to ASD: Evidence from molecular, in silico, and meta-analysis approaches. *Mol. Biol. Rep.* **49**(9), 8449–8460. https://doi.org/10.1007/s11033-022-07663-z (2022).
67. Pejaver, V. et al. Inferring the molecular and phenotypic impact of amino acid variants with MutPred2. *Nat. Commun.* **11**(1), 5918. https://doi.org/10.1038/s41467-020-19669-x (2020).
68. Capriotti, E., Fariselli, P. & Casadio, R. I-Mutant2. 0: Predicting stability changes upon mutation from the protein sequence or structure. *Nucleic Acids Res.* **33**(suppl_2), W306–W310. https://doi.org/10.1093/nar/gki375 (2005).
69. Hussein, Z. A. & Al-Kazaz, A. A. Bioinformatics evaluation of CRISP2 gene SNPs and their impacts on protein. *Iraqi J. Agri Sci.* **54**(2), 369–377 (2023).
70. Yariv, B. et al. Using evolutionary data to make sense of macromolecules with a face-lifted ConSurf. *Protein Sci.* **32**(3), e4582. https://doi.org/10.1002/pro.4582 (2023).
71. Szklarczyk, D. et al. The STRING database in 2023: Protein–protein association networks and functional enrichment analyses for any sequenced genome of interest. *Nucleic Acids Res.* **51**(D1), D638–D646. https://doi.org/10.1093/nar/gkac1000 (2023).

Author contributions

S.M. Conception, data acquisition, analysis, manuscript drafting, critical revision, final approval; H.M. Conception, data acquisition, analysis, manuscript drafting, critical revision, final approval; M.W. Data acquisition, Analysis, final approval; Z.K. Analysis, manuscript drafting, critical revision, final approval; S.W.A. Data acquisition, analysis, final approval; K.R. Data acquisition, analysis, final approval.

Declarations

Competing interests

The authors declare no competing interests.

Additional information

Supplementary Information The online version contains supplementary material available at https://doi.org/10.1038/s41598-024-83254-1.

Correspondence and requests for materials should be addressed to H.M. or Z.K.